RESEARCH ARTICLE • OPEN ACCESS

Cost-effectiveness with Optimal Strategies for Enhancing Population Birth Rate Trends in Japan

Pulak Kundu and Uzzwal Kumar Mallick

Volume 6, Issue 2, Pages 71–87, June 2025

Received 20 March 2025, Revised 16 April 2025, Accepted 2 May 2025, Published Online 14 June 2025

To Cite this Article : P. Kundu and U. K. Mallick,“Cost-effectiveness with Optimal Strategies for Enhancing Population Birth Rate Trends in Japan”, *Jambura J. Biomath*, vol. 6, no. 2, pp. 71–87, 2025, *https://doi.org/10.37905/jjbm.v6i2.30983*

JOURNAL INFO • JAMBURA JOURNAL OF BIOMATHEMATICS

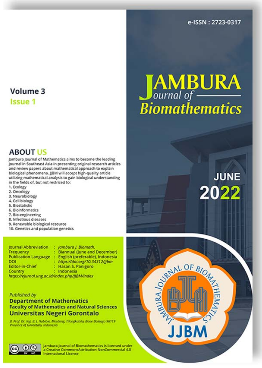

Homepage	:	http://ejurnal.ung.ac.id/index.php/JJBM/index
Journal Abbreviation	:	Jambura J. Biomath.
Frequency	:	Quarterly (March, June, September and December)
Publication Language	:	English
DOI	:	https://doi.org/10.37905/jjbm
Online ISSN	:	2723-0317
Editor-in-Chief	:	Hasan S. Panigoro
Publisher	:	Department of Mathematics, Universitas Negeri Gorontalo
Country	:	Indonesia
OAI Address	:	http://ejurnal.ung.ac.id/index.php/jjbm/oai
Google Scholar ID	:	XzYgeKQAAAAJ
Email	:	editorial.jjbm@ung.ac.id

Jambura Journal of Biomathematics, Volume 6, Issue 2, Pages 71–87, June 2025 https://doi.org/10.37905/jjbm.v6i2.30983

Research Article

Cost-effectiveness with Optimal Strategies for Enhancing Population Birth Rate Trends in Japan

Pulak Kundu[1] and **Uzzwal Kumar Mallick**[2,*]

[1]*Department of Computer Science and Engineering, Northern University of Business and Technology Khulna, Khulna-9100, Bangladesh*
[2]*Mathematics Discipline, Khulna University, Khulna-9208, Bangladesh*

ARTICLE HISTORY
Received 20 March 2025
Revised 16 April 2025
Accepted 2 May 2025
Published 14 June 2025

KEYWORDS
Awarness program
Aging people
Cost efficiency
Fertility rate
Incentives
Workaholism

ABSTRACT. *Japan faces one of the major challenges as its declining birth rate and aging population threaten long-term demographic and economic stability. To address this challenge, a mathematical model with optimal control has been formulated, employing awareness programs and incentives to maximize population growth at minimal policy costs. Along with analyzing the model's positivity, boundedness, existence of a unique solution, and stability at equilibrium points, the optimal control was characterized using Pontryagin's Maximum Principle. Using the forward-backward sweep method, the numerical simulation demonstrated that the objective is maximized by applying awareness programs and incentives at full capacity until 2042 and 2046, respectively, before gradually reducing them. Then, a cost-effectiveness analysis was conducted to determine the most efficient approach, revealing that awareness programs are more cost-effective than the alternative strategy. Therefore, the findings of this study provide valuable guidance for policymakers to develop practical, cost-effective strategies that address Japan's demographic challenges and promote sustainable population growth for society.*

1. Introduction

Japan, a country known for its scientific breakthroughs, strong economic base, and high quality of life, is presently confronting a huge population crisis. The nation's population growth has slowed, owing mostly to a decreased birth rate, resulting in an aging population. This tendency has major ramifications for Japan's economic and social structures, compromising its sustainability over the long term.

Japan's progress after the extensive destruction of World War II is a remarkable achievement, marked by rapid economic growth, groundbreaking technological innovations, and a significant increase in its global influence across various sectors [1]. By the 1980s, Japan had emerged as one of the world's leading economic powers, boasting a strong industrial base, a robust export market, and an increasingly affluent population [2]. In recent decades, however, this progress has been overshadowed by a persistent decline in the birth rate, which has significantly impacted the demographic landscape of the nation [3] and regrettably, in recent years, the annual number of births has been gradually falling below the number of deaths, as shown in Figure 1a. As of 2023, demographic statistics from the Ministry of Health, Labour, and Welfare reveal that Japan's fertility rate dropped to a record low of 1.20 children per woman, marking the eighth consecutive year of decline (see Figure 1b), with all 47 prefectures seeing decreases, including Tokyo falling below 1.0 for the first time (0.99) and Saitama, Chiba, and Kanagawa recording rates below 1.2 [4]. In 2024, Japan recorded a historic low of 720,988 births, marking the ninth consecutive year of declining birth rates. This figure represents a 5% decrease from the previous year and is the lowest since records began in the Meiji era in 1899 [5]. Concomitantly, Japan is witnessing an increase in the elderly population to 36.25 million, with citizens aged 65 and above comprising one-third of the total population, as declared by Japan's Ministry of Internal Affairs and Communications [6]. This alarming trend is part of a broader demographic shift, as Japan's population has been steadily declining from a peak of approximately 128 million in 2010 to below 124 million in 2024 (see Figure 1c) [7]. Declining birth rates and aging populations have become critical challenges for developed countries such as Japan, South Korea, and Italy, posing significant economic and social concerns, as by 2050, Japan's population is expected to decrease from 122 million to 100 million, while South Korea's will shrink from 51.6 million to 46 million [8]. This demographic shift, influenced by technological advancements and the increasing busyness of work, has led to a decline in marriage rates and a reluctance to have children in Japan, resulting in a shrinking working-age population and an aging population [9]. While a smaller population may reduce employment and production, strategies like increased capital intensity, productivity improvements, and higher labour force participation could help mitigate the impact on per capita income [10]. Additionally, the Japanese government acknowledged these demographic changes during Respect for the Aged Day, highlighting the growing importance of the elderly in national policy [11].

According to Rahman [12], the Japanese government is introducing different policies to ease the burden on Tokyo, includ-

*Corresponding Author.

Email : *mallickuzzwal@math.ku.ac.bd* (U. K. Mallick)
Homepage : http://ejurnal.ung.ac.id/index.php/JJBM/index / E-ISSN : 2723-0317

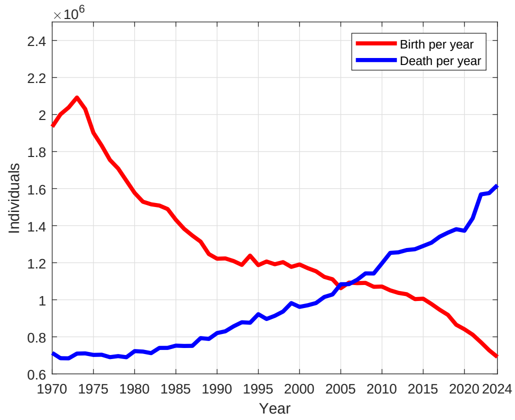

(a)

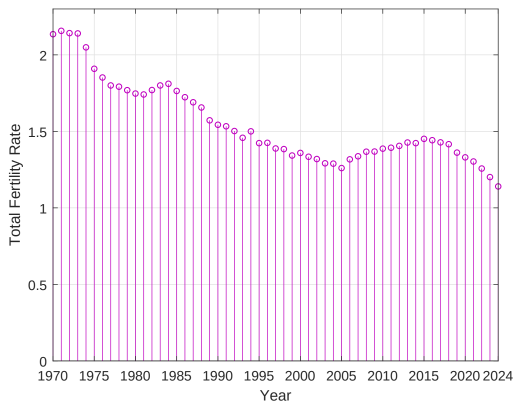

(b)

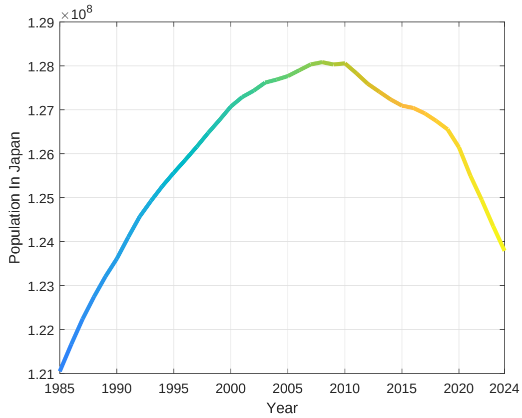

(c)

Figure 1. (a) Yearly birth and death trends in Japan from 1970 to 2024, showing a decline in birth rates and a rise in death rates over time. (b) Total fertility rate (TFR) in Japan from 1970 to 2024, highlighting a gradual decline with slight fluctuations in recent decades. (c) Japan's population grew until the mid-2000s, then declined monotonically, with a slight rise from 2005 to 2010 due to migration despite the death rate remaining higher compared to the birth rate [?].

ing offering up to 1 million yen per child for families relocating from the metropolitan area, with the program set to begin in April 2023. Families with two parents and two children under 18 who establish a business in another region will receive ¥500,000. Additionally, the government will provide free medical care for schoolchildren until age 8. Furthermore, mathematical models are becoming valuable tools for analyzing the impact of natural events on regions and populations [13, 14]. Among these, mathematical modeling using systems of ordinary differential equations has been extensively employed to study this phenomenon including disease dynamics, ecological processes [15, 16]. In 2022, a multi-regional Leslie matrix model has been developed for analyzing the effects of fertility rates and interregional migration on population dynamics, and was observed that migration from urban areas to high-fertility regions and fertility rates in urban areas significantly impact population growth, especially for people under 30 and over 30 [17]. After, Oliver [18] investigated the relationship between Japan's aging population and immigration from 1975 to 2019, finding that a decrease in the 60–64 age group and an increase in those aged 65+ are linked to a rise in foreign residents. Again, a newly proposed mathematical model has been formulated by Kundu and Mallick [19] using ordinary differential equations, considering birth rate as a variable, to analyze Japan's declining birth rate and aging population, and the findings emphasize the urgency of awareness campaigns and policy interventions to sustain population growth. Again, a research has been conducted to investigate Japan's aging process using SAPP (The Web System of Small Area Population Projections) for Japan data, identifying four stages of population aging and finding that areas with higher elderly populations experience stage shifts earlier, driven by long-term fertility decline and youth migration, with the results suggesting that similar trends will occur in other developed countries after their demographic transitions [20]. Besides, Respatiadi et al. [21] examined Japan's demographic crisis, emphasizing the long-standing shoushika phenomenon of declining birth rates and a growing elderly population, attributing it to post-World War II development strategies and highlighting the urgent need for strategic solutions to address the issue. Not only in Japan, but also in other developed countries, low birth rates and aging populations pose challenges as Kim et al. [22] analyzed South Korea's population imbalance, predicting depopulation risks for 30+ cities by 2072 and highlighting public transportation's role in mitigating regional decline, offering insights for sustainable development. Cost-effectiveness is increasingly crucial for ensuring quality, sustainability, and efficient resource use, especially in finding better strategies. In this track, Samui et al. [23] highlighted the effectiveness of self-monitoring, increased awareness, and improved treatment as cost-effective non-pharmaceutical and therapeutic strategies in controlling COVID-19 transmission through a compartmental model and optimal control analysis. Again, the study by Igbo et al. [24] explored strategies for continuous professional development in healthcare to improve cost-effective, high-quality, and sustainable healthcare delivery, emphasizing the need for a digital ecosystem in South Africa.

However, following a comprehensive review of the existing literature, this study employs optimal control theory to devise strategies aimed at maximizing profitability in efforts to increase Japan's population through birth rate enhancement. Furthermore, a cost-effectiveness analysis is conducted to identify the most economically viable strategy for achieving this objective.

The rest of the paper is structured as follows: Section 2 introduces the mathematical model and optimal control problem formulation. In Section 3, we conduct a mathematical analysis of the model. The characterization of the optimal control problem is discussed in Section 4. Section 5 presents the results of the numerical simulations and the discussion of various cases. The next step, Section 6, evaluates different control strategies for cost-effectiveness. Finally, Section 7 provides a summary and conclusion of the findings.

2. Formulation for Optimal Control Problem

In a previous study Kundu and Mallick [19], a mathematical model was newly proposed using a system of ordinary differential equations to analyze the critical issue of Japan's declining birth rate. By exploring various demographic factors and their impact on population dynamics, the study aimed to provide actionable insights for policymakers to address the pressing challenges of an aging population and a shrinking workforce.

In the above study, a mathematical model has been proposed using the two state variables, the population in Japan $(N(t))$ and the birth rate $(B(t))$.

$$\frac{dN}{dt} = \alpha BN - \gamma N^2 - \mu N,$$
$$\frac{dB}{dt} = \tau + \sigma B - \xi B - \omega B - \delta B,$$

where α represents the population growth rate influenced by immigration and birth rate, while the logistic growth rate and natural death rate are denoted by γ and μ, respectively. Additionally, τ and σ represent the rates of awareness programs and incentives, respectively, while ξ, ω, and δ correspond to the decline in birth rate attributed to workaholism, technological advancements, and price inflation, accordingly. Regrettably, this study does not incorporate a control approach to optimize population growth while minimizing the cost of strategies, such as implementing awareness programs and incentive schemes—one of the key challenges associated with this issue. Addressing this limitation necessitates the application of two optimal control strategies to identify the minimal cost function.

If we provide a lower amount of incentives and arrange fewer awareness programs, the rise in the population can be less, and the associated cost can also be reduced. However, during this time, it is important to evaluate whether the objective of increasing the population is being achieved or not. To address this, we will apply the concept of optimal control in this study. Within this framework, the optimal control problem is formulated by considering two time-dependent control variables $u_1(t)$ and $u_2(t)$, specifically, $u_1(t)$ defines the execution of awareness programs while $u_2(t)$ regulates the allocation of incentives.

Generally, population growth is influenced by higher birth rates and immigration, as individuals seek better opportunities. However, this growth is constrained by resource depletion from intraspecies competition, while natural deaths contribute to population decline. In addition, birth rates, a critical factor in population growth, can be boosted through public awareness campaigns about the negative impacts of population decline on national development, which are controlled by $u_1(t)$. In countries like Japan, high career demands and the rising costs of raising a family, exacerbated by inflation, discourage family planning. To address this, the government may offer incentives to encourage higher birth rates, with the allocation of these incentives controlled by $u_2(t)$. By effectively managing these controls, the following system of nonlinear differential equations (for flow diagram, see Figure 2) seeks to maximize Japan's population while optimizing the associated costs.

$$\frac{dN(t)}{dt} = \alpha B(t)N(t) - \gamma N^2(t) - \mu N(t), \tag{1}$$
$$\frac{dB(t)}{dt} = u_1(t)\tau + u_2(t)\sigma B(t) - \xi B(t) - \omega B(t) - \delta B(t), \tag{2}$$

with the initial conditions $N(0) = N_0$ and $B(0) = B_0$.

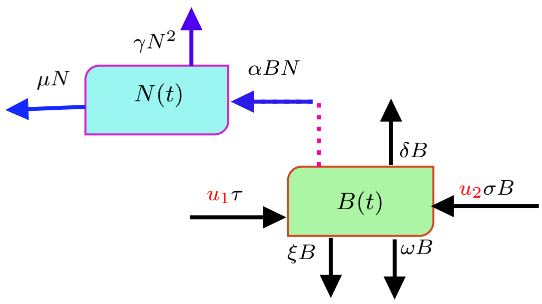

Figure 2. Flow Diagram of the eqs. (1) and (2)

Our goal is to identify control strategies that minimize the costs for the government and policymakers associated with awareness programs and incentives, while maximizing the population growth in Japan. We have used the square of the control variables to calculate the policymaking costs, as this approach not only optimizes population growth but also helps stabilize the optimal control state. Therefore, we adopt a linear approach in this context. Since our objective is to maximize the population, the following functional objective is chosen:

$$\textbf{Maximize } J(u_1(t), u_2(t)) = \int_{t_s}^{t_f} \Big[A_1 N(t) - A_2 u_1^2(t) - A_3 u_2^2(t)\Big] dt. \tag{3}$$

The policymaking cost is a non-linear function involving $u_1(t)$ and $u_2(t)$, which are quadratic cost functions that ensure concavity. Since $u_1(t)$ and $u_2(t)$ are constrained, the right-hand sides of eqs. (1) and (2) are linearly bounded in relation to $u_1(t)$ and $u_2(t)$ [Subsection: 3.2]. These boundaries provide the compactness necessary for the existence of optimal control, as outlined by Fleming and Rishel [25]. Pontryagin's maximum principle, discussed in Pontryagin et al. and Vinter [26, 27], is applied to the model, allowing us to simulate the optimal solution. Furthermore, the parameters A_1, A_2, and $A_3 \geq 0$ are used as weights to determine the optimal cost. Our objective is to identify the control profiles that meet the following condition:

$$J\Big(u_1^*(t), u_2^*(t)\Big) = \max\Big\{J(u_1(t), u_2(t))|0 \leq u_1(t), u_2(t) \leq 1\Big\}.$$

Hence, our newly proposed eqs. (1) and (2) can be formulated using objective functions eq. (3) in the optimal control problem as

$$(P)\begin{cases} \textbf{Maximize} \quad J\left(x(t), u(t)\right) = \displaystyle\int_{t_s}^{t_f} L(t, x(t), u(t))dt \\ \text{subjected to} \\ \dot{x}(t) = f(x(t)) + g(x(t))u(t), \quad \forall t \in [t_s, t_f] \\ u(t) \in \mathcal{U}, \quad \forall t \in [t_s, t_f] \\ x(0) = x_0 \end{cases}$$

where,

$$\begin{aligned} x(t) &= \begin{bmatrix} N(t) \\ B(t) \end{bmatrix}, \\ L &= (t, x(t), u(t)) \\ &= A_1 N(t) - A_2 u_1^2(t) - A_3 u_2^2(t), \\ f(x) &= \begin{bmatrix} \alpha B(t)N(t) - \gamma N^2(t) - \mu N(t) \\ -\xi B(t) - \omega B(t) - \delta B(t) \end{bmatrix}, \\ u(t) &= \begin{bmatrix} u_1(t) \\ u_2(t) \end{bmatrix}, \\ g(x) &= \begin{bmatrix} 0 & 0 \\ \tau & \sigma B(t) \end{bmatrix}. \end{aligned}$$

3. Mathematical Analysis

In order to demonstrate the mathematical and biological significance of the proposed eqs. (1) and (2), it is vital to provide evidence of the existence, non-negativity, and bounded nature of its solutions.

3.1. Positivity of the model

Lemma 1. *If $N(0) \geq 0$ and $B(0) \geq 0$, then $N(t)$ and $B(t)$ will remain non-negative for all $t\epsilon[0, T]$ within R_2^+ where $T > 0$.*

Proof. From the eq. (2), we can write

$$\begin{aligned} \frac{dB(t)}{dt} &= \tau u_1 + (u_2\sigma - \xi - \omega - \delta)B(t) \\ \frac{dB(t)}{B(t)} &\geq \Big(u_2\sigma - \xi - \omega - \delta\Big)dt \end{aligned}$$

After integration, we find that

$$\begin{aligned} B &\geq B_0 e^{(u_2\sigma - \xi - \omega - \delta)t} \\ \therefore B(t) &\geq B_0 e^{(u_2\sigma - \xi - \omega - \delta)t} > 0 \end{aligned}$$

Thus, we conclude that $B(t) > 0$. Similarly, it can be observed from eq. (2) that

$$\therefore N(t) = e^{-\mu t + \int (\alpha NB - \gamma N)dt} > 0$$

□

3.2. Boundedness of the model

Lemma 2. *All the solution $(N(t), B(t))$ of the eqs. (1) and (2) are bounded.*

Proof. Let $S(t)$ be the sum of the solutions $N(t)$ and $B(t)$ in our proposed model. That means,

$$S(t) = N(t) + B(t) \tag{4}$$

$$\frac{dS}{dt} + \Omega S = \frac{dN}{dt} + \frac{dB}{dt} + \Omega(N + B) \tag{5}$$

Putting the values we get,

$$\begin{aligned} \therefore \frac{dS}{dt} + \Omega S = \alpha NB - \gamma N^2 - \mu N + \ u_1\tau + u_2\sigma B - \xi B \\ - \omega B - \delta B + \Omega N + \Omega B. \end{aligned} \tag{6}$$

Let us now have a look at a function of $h(x, y)$ that is put out in the following manner:

$$h(x, y) = \alpha xy - \gamma x^2 - \mu x + u_1\tau + u_2\sigma y - \xi y - \omega y - \delta y + \Omega x + \Omega y. \tag{7}$$

Here, $h(x, y)$ is a surface in the domain $0 \leq x \leq T_1$ and $0 \leq y \leq T_2$. Now, we want to analyze the local maximum or minimum at the critical point by applying the theorem presented in Anton et al. [28].

For this reason, let us consider (x_0, y_0) is a critical point of $h(x, y)$. So, we have to determine the value of $Z = h_{x_0x_0}h_{y_0y_0} - h_{x_0x_0}h_{x_0y_0}^2$. Thus we get

$$Z = -(-2\gamma)(\alpha)^2 = 2\gamma\alpha^2 > 0. \tag{8}$$

Due to the fact that $Z > 0$ and $h_{x_0x_0} = -2\gamma < 0$ with $h_{y_0y_0} = 0, h_{x_0y_0} = \alpha$, $h(x, y)$ holds a local maximum. Hence, according to the theorem mentioned in Anton et al. [28], taking the maximum value ψ of $h(N, B)$ to be taken into consideration eq. (6) states that,

$$\lim_{t\to\infty} Sup\{S(t)\} \leq \frac{\psi}{\Omega}. \tag{9}$$

This leads to the conclusion that the solutions of the states $N(t)$ and $B(t)$ of the system remain within bounded limits. □

3.3. Existence and uniqueness of the model solution

Theorem 1 (Existence and uniqueness of the model solution). *Let D be a domain that satisfies the Lipschitz condition. Then, for all non-negative initial conditions, the system's solutions exist and remain unique for every $T \geq 0$ within the domain D.*

Proof. The theorem described in Sowole et al. [29] and Kundu and Mallick [30] has shown that it is necessary to adhere to the suggested Lipschitz criteria in order to ensure the existence and uniqueness of a solution inside a domain, denoted as D. Let,

$$f(N,B) = \frac{dN}{dt} = \alpha BN - \gamma N^2 - \mu N, \tag{10}$$

$$g(N,B) = \frac{dB}{dt} = u_1\tau + u_2\sigma B - \xi B - \omega B - \delta B. \tag{11}$$

Using above system's equation, we get

$$\frac{\partial f}{\partial N} = \alpha B - 2\gamma N - \mu, \quad \left|\frac{\partial f}{\partial N}\right| = \left|\alpha B - 2\gamma N - \mu\right| \leq \frac{\psi}{\Omega} < \infty, \tag{12}$$

$$\frac{\partial f}{\partial B} = 0, \qquad \left|\frac{\partial f}{\partial B}\right| = 0 < \infty. \tag{13}$$

Again,

$$\frac{\partial g}{\partial N} = 0, \qquad \left|\frac{\partial g}{\partial N}\right| = 0 \leq \frac{\nu}{\Lambda} < \infty, \tag{14}$$

$$\frac{\partial g}{\partial B} = u_2\sigma - \xi - \omega - \delta, \quad \left|\frac{\partial g}{\partial B}\right| = \left|u_2\sigma - \xi - \omega - \delta\right| \leq \frac{\psi}{\Omega} < \infty. \tag{15}$$

Hence, we have demonstrated that all partial derivatives are both continuous and bounded, ensuring compliance with the Lipschitz condition. Consequently, following the theory outlined in Sowole et al. [29], the eqs. (1) and (2) exhibits a unique solution within the region D. □

3.4. Equilibrium points

After solving the following equations,

$$f(N,B) = \alpha BN - \gamma N^2 - \mu N = 0, \tag{16}$$

$$g(N,B) = u_1(t)\tau + u_2(t)\sigma B - (\xi + \omega + \delta)B = 0, \tag{17}$$

we obtain two non-negative equilibrium points as follows:

- Axial equilibrium point: $E_1 = \left(0, \dfrac{u_1(t)\tau}{\kappa}\right)$, exists if $\delta + \omega + \xi > u_2(t)\sigma$, where $\kappa = \delta - u_2(t)\sigma + \omega + \xi$.
- Interior equilibrium point: $E_2 = \left(\dfrac{u_1(t)\alpha\tau - \mu\kappa}{\gamma\kappa}, \dfrac{\tau}{\kappa}\right)$, exists if $u_1(t)\alpha\tau + u_2(t)\mu\sigma > \mu(\xi+\omega)$ and $\delta+\omega+\xi > u_2(t)\sigma$.

3.5. Stability analysis

Theorem 2 (Stability of the Axial Equilibrium Point). *The axial equilibrium point E_1 of the dynamical system is unstable.*

Proof. The jacobian matrix for the system based on the eqs. (16) and (17) would be

$$J = \frac{\partial(f,g)}{\partial(N,B)} = \begin{pmatrix} \frac{\partial f}{\partial N} & \frac{\partial f}{\partial B} \\ \frac{\partial g}{\partial N} & \frac{\partial g}{\partial B} \end{pmatrix}$$

$$J = \begin{pmatrix} \alpha B - 2\gamma N - \mu & \alpha N \\ 0 & u_2(t)\sigma - \xi - \omega - \delta \end{pmatrix}$$

For the equilibrium point$E_1 = \left(0, \frac{\tau}{\kappa}\right)$, we obtain

$$J_{|E_1} = \begin{pmatrix} \alpha\frac{\tau}{\kappa} - \mu & 0 \\ 0 & u_2(t)\sigma - \xi - \omega - \delta \end{pmatrix} \tag{18}$$

$$\therefore J_{|E_1} = \begin{pmatrix} \alpha\frac{\tau}{\kappa} - \mu & 0 \\ 0 & -\kappa \end{pmatrix} \tag{19}$$

where $\kappa = \xi + \omega + \delta - u_2(t)\sigma$ and $u_2(t)$ is always positive as it varies from only $[0,1]$. Therefore, the characteristic equation for the equilibrium point E_1 would be

$$\left|J_{|E_1} - \lambda I\right| = 0, \tag{20}$$

$$\begin{vmatrix} \alpha\frac{\tau}{\kappa} - \mu - \lambda & 0 \\ 0 & -\kappa - \lambda \end{vmatrix} = 0, \tag{21}$$

$$\therefore \lambda_1 = \frac{\alpha\tau - \mu\kappa}{\kappa}, \lambda_2 = -\kappa. \tag{22}$$

It is easily observed that λ_2 is negative, while λ_1 can vary (either positive or negative). Under the conditions in the subsection entitled "Equilibrium points", λ_1 must be positive to ensure a positive equilibrium point. Hence the equilibrium point E_1 is a saddle point, and the system is unstable at this point. □

Theorem 3 (Stability of the Interior Equilibrium Point). *The dynamical of eqs. (1) and (2) is asymptotically stable at the point E_2 when $\alpha u_1(t)\tau + \mu u_2(t)\sigma > \mu(\xi+\omega)$ and $\delta + \omega + \xi > u_2(t)\sigma$, otherwise unstable.*

Proof. The Jacobin matrix at the equilibrium point becomes,

$$J_{|E_2} = \begin{pmatrix} \alpha\frac{\tau}{\kappa} - 2\gamma\frac{\alpha\tau-\mu\kappa}{\gamma\kappa} - \mu & \alpha\frac{\alpha\tau-\mu\kappa}{\gamma\kappa} \\ 0 & -\kappa\frac{\tau}{\kappa} \end{pmatrix}, \tag{23}$$

where $\kappa = \delta - u_2(t)\sigma + \omega + \xi$.
After solving the characteristic equation obtained from equilibrium point E_2, we get two values of λ

$$\lambda_1 = -\kappa, \lambda_2 = -\frac{(\alpha\tau - \mu\kappa)}{\kappa}. \tag{24}$$

Under the conditions mentioned previously $\Big(\alpha\tau + \mu u_2(t)\sigma > \mu(\xi+\omega)$ and $\delta + \omega + \xi > \sigma u_2(t)\Big)$, all eigenvalues (λ_1, λ_2) are negative, ensuring that the system is asymptotically stable at that equilibrium point. □

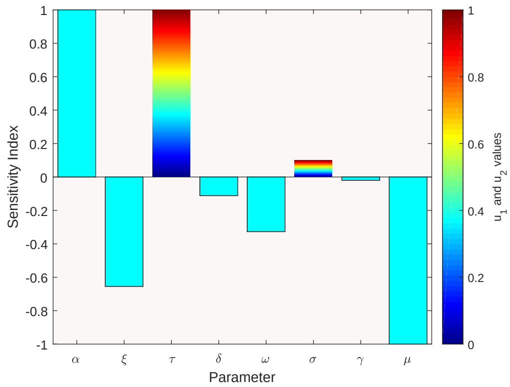

Figure 3. Effects of parameter variations on R_0

Table 1. Parameter value and their descriptions [19]

Symbol	Parameter's Description	Value $(year^{-1})$
α	rate of population based on by immigration and birth rate	0.001
γ	logistic growth rate of Japan human population	3.0×10^{-10}
μ	natural death rate	0.012
τ	the increasing birth rate by making awareness program	0.0056
σ	rising birth rate as a result of incentives	0.0012
ξ	declining birth rate caused by workaholism (business in work)	0.0083
ω	decreasing birth rate due to technological progress	0.00415
δ	Decreasing peace in birth rate resulting from price inflation	0.00142

3.6. Sensitivity analysis

Sensitivity analysis plays a vital role in identifying the parameters that most influence the model outcomes for the Japanese population to support more effective and informed policy decisions, particularly through the future status represented by the basic reproduction number $R_0 = \frac{\alpha\frac{\tau}{\kappa}}{2\gamma\frac{\alpha\tau-\mu\kappa}{\gamma\kappa}+\mu}$. This analysis can be done using sensitivity indices. These indices provide a quantitative measure of the responsiveness of a state variable to variations in a specific parameter. Following the approach described in Omoloye and Adewale [31], the sensitivity index is defined using partial derivatives as:

$$\Lambda_x^q = \frac{\partial x}{\partial q} \times \frac{q}{x},$$

where x represents the state variable and q is the parameter under consideration. Particularly,

$$\begin{aligned}
\Lambda_\alpha^{R_0} &= \frac{\partial R_0}{\partial \alpha} \times \frac{\alpha}{R_0} & \Lambda_\delta^{R_0} &= \frac{\partial R_0}{\partial \delta} \times \frac{\delta}{R_0} \\
&= 1 & &= -0.1121 \\
\Lambda_\tau^{R_0} &= \frac{\partial R_0}{\partial \tau} \times \frac{\tau}{R_0} & \Lambda_\omega^{R_0} &= \frac{\partial R_0}{\partial \omega} \times \frac{\omega}{R_0} \\
&= u_1(t) * 1 & &= -0.3275 \\
\Lambda_\sigma^{R_0} &= \frac{\partial R_0}{\partial \sigma} \times \frac{\sigma}{R_0} & \Lambda_\xi^{R_0} &= \frac{\partial R_0}{\partial \xi} \times \frac{\xi}{R_0} \\
&= u_2(t) * 0.0947 & &= -0.6551 \\
\Lambda_\gamma^{R_0} &= \frac{\partial R_0}{\partial \gamma} \times \frac{\gamma}{R_0} & \Lambda_\mu^{R_0} &= \frac{\partial R_0}{\partial \mu} \times \frac{\mu}{R_0} \\
&= -5 \times 10^{-8} & &= -1
\end{aligned}$$

where the value of control parameters $u_1(t)$ and $u_2(t)$ varies from 0 to 1.

From Figure 3, it is observed that a variety of factors influence the sensitivity index within our system. Notably, the parameters (τ, σ) associated with providing incentives and organizing awareness programs exhibit positive sensitivity indices. This implies that boosting these initiatives could significantly contribute to increasing Japan's population in the future. In contrast, parameters such as ξ and δ, which are linked to workaholism and price inflation, show negative sensitivity indices—highlighting the need to mitigate these factors to help reverse Japan's population decline.

4. Characterization of the Optimal Control Problem

To find the optimal solution, we will analyze the necessary optimality conditions of the maximum principle [26]. At first, the Hamiltonian function for maximizing $J(u_1(t), u_2(t))$ is defined as follows:

$$H[x(t), p(t), u(t)] = \lambda L(x(t), u(t)) + \langle p(t), f(x), \quad \lambda \in \mathbb{R} \\ + g(x)u(t)\rangle \tag{25}$$

where, the adjoint variables are denoted by $p = (p_N, p_B)$. Assume that $(x^*(t), u^*(t))$ is an optimal solution. Therefore, from the maximum principle, there appears a scalar $\lambda \geq 0$, an absolutely continuous function $p(t)$, with the time argument $\lfloor t \rfloor$ denoting the evaluation along the optimal solution:

$$i.\ \max\{|p(t)| : t \in [t_s, t_f]\} + \lambda > 0 \tag{26}$$

$$ii.\ \dot{p}(t) = -H_x[x] = -\lambda L_x[t] - \langle p(t), f_x(t) + g_x(t)u^*(t)\rangle \tag{27}$$

$$iii.\ p(t_f) = (0, 0, 0) \tag{28}$$

$$iv.\ H(x^*(t), p(t), u^*(t)) = \max_u\{H(x^*(t), p(t), u(t)) : 0 \leq u(t) \leq 1\} \tag{29}$$

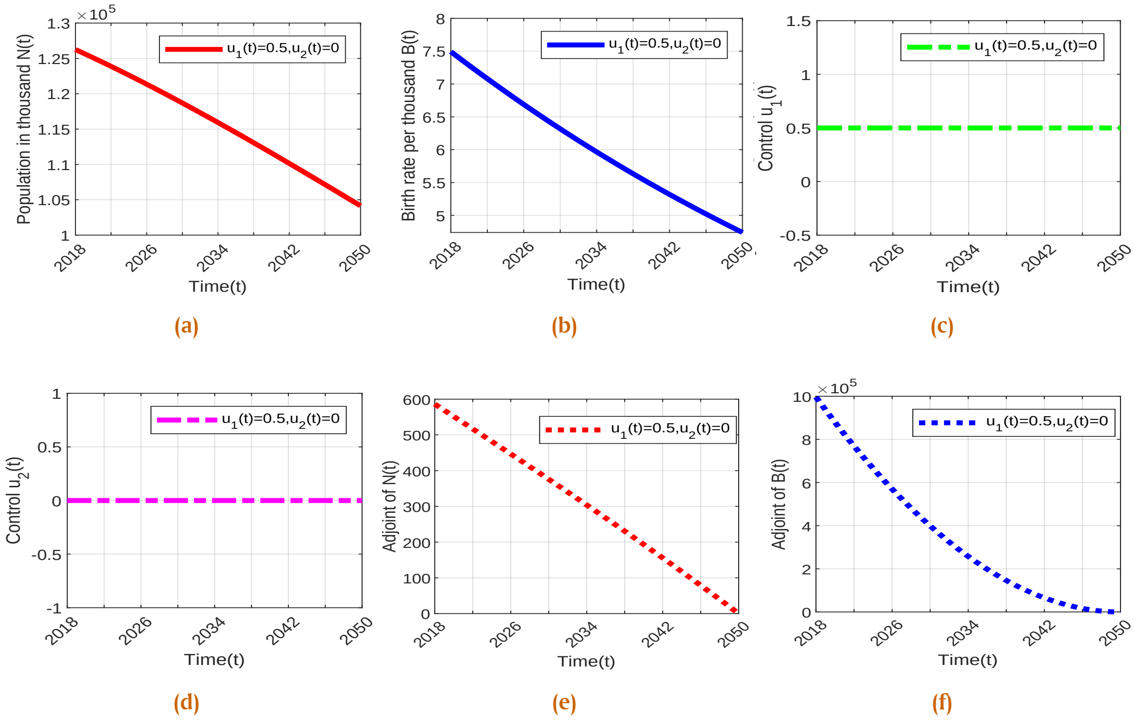

Figure 4. When implementing a control strategy that allocates half the capacity to organizing awareness programs without providing incentives, as depicted in (c) and (d), the corresponding simulated solution curves for population and birth rate are displayed in (a) and (b), respectively, with their associated adjoint profiles shown in (e) and (f). [Case-1]

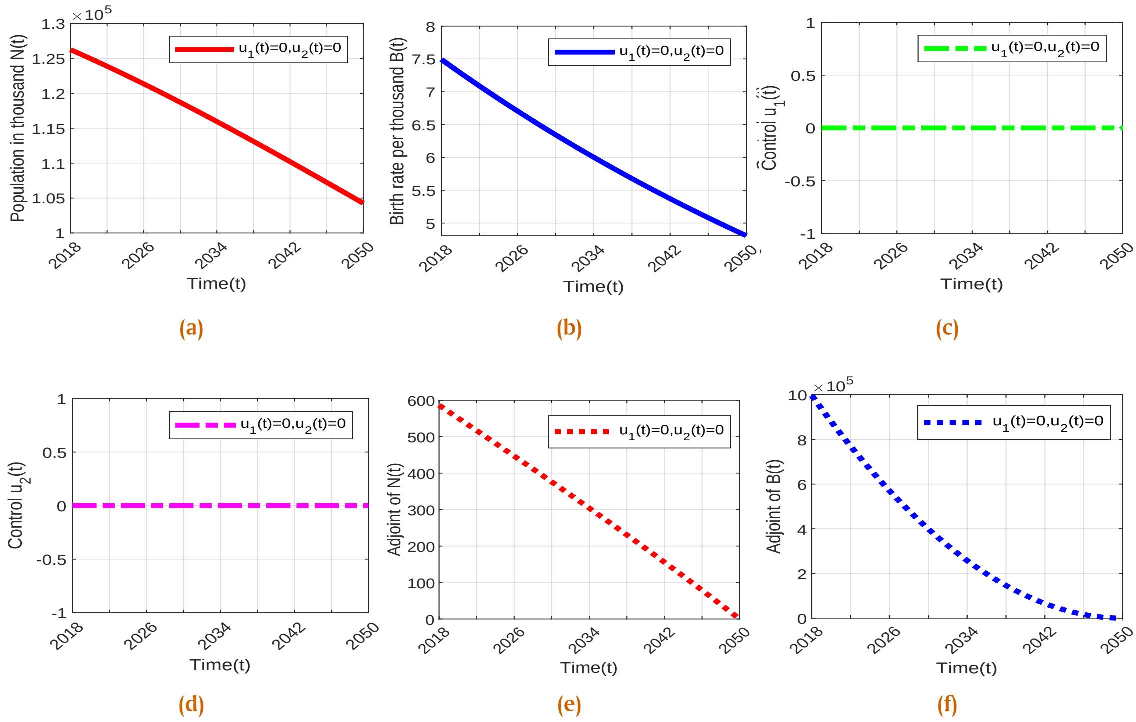

Figure 5. In the absence of awareness programs and incentives, as shown in (c) and (d), the resulting simulated solution curves for population and birth rate unfold in (a) and (b), with their corresponding adjoint profiles elegantly captured in (e) and (f). [Case-2]

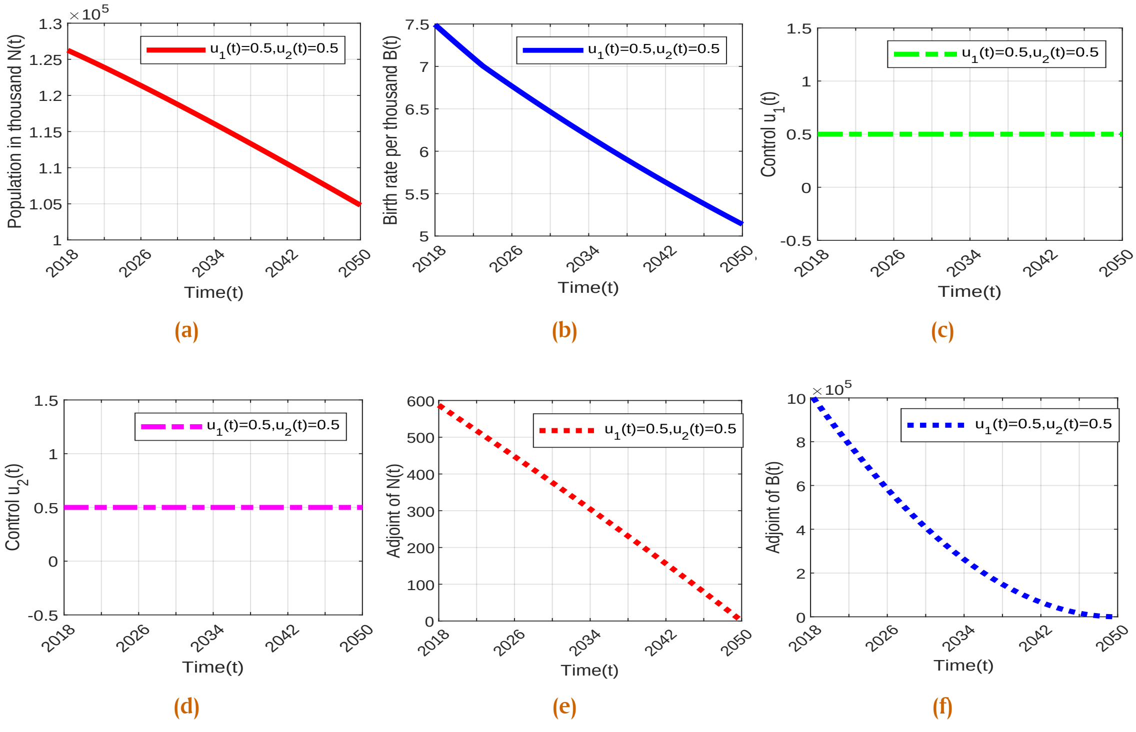

Figure 6. The solution curves from simulation for population and birth rate, shown in (a) and (b), respectively, result from allocating 50% of the total capacity to organizing awareness programs and providing incentives, as depicted in (c) and (d), while the corresponding adjoint profiles are displayed in (e) and (f). [Case-3]

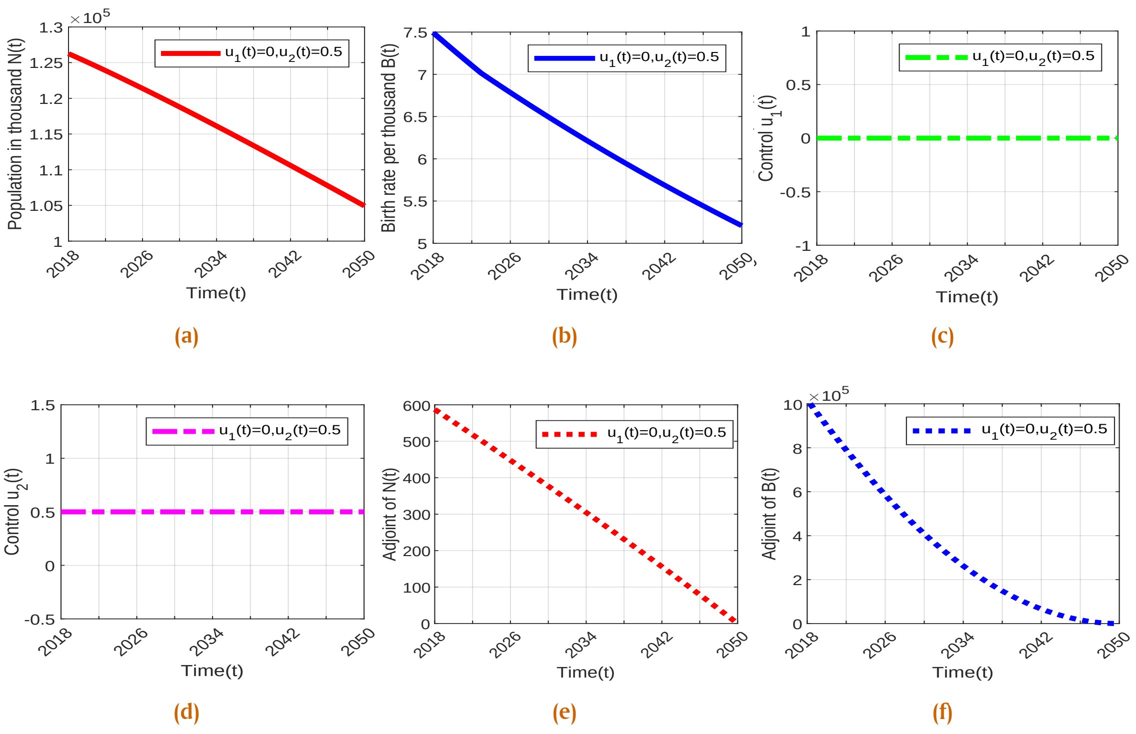

Figure 7. The adjoint profiles, presented in (e) and (f), result from allocating 50% of the total capacity to incentives without arranging awareness programs (as shown in (c) and (d)), with the simulated solution curves for population and birth rate displayed in (a) and (b), respectively. [Case-4]

The adjoint eq. (27) with adjoint variables $p = (p_N, p_B)$ in normal form $(i.e.\lambda = 1)$ are explicitly provided by the following equation:

$$\dot{p_N} = -\frac{\partial H}{\partial N},$$
$$\therefore \dot{p_N} = -A_1 - \alpha p_N B(t) + 2\gamma p_N N(t) + \mu p_N, \tag{30}$$
$$\dot{p_B} = -\frac{\partial H}{\partial B},$$
$$\therefore \dot{p_B} = -\alpha p_N N(t) - u_2(t)\sigma p_B + \xi p_B + \omega p_B + \delta p_B, \tag{31}$$

where

$$H = A_1 N(t) - A_2 u_1^2(t) - A_3 u_2^2(t) + p_N\Big\{\alpha B(t)N(t) - \gamma N^2(t) - \mu N(t)\Big\} + p_B\Big\{u_1(t)\tau + u_2(t)\sigma B(t) - \xi B(t) - \omega B(t) - \delta B(t)\Big\}.$$

Again, We deduce from eq. (29) and get an explicit characterization of optimal control pair in normal form $i.e(\lambda = 1)$ given in terms of the multipliers $p = (p_B, p_E)$ and we get,

$$\begin{array}{ccc} \langle p, f(x^*(t)) + g(x^*(t))u^*(t)\rangle & \geq & \langle p, f(x^*(t)) + g(x^*(t))u(t)\rangle \\ +L(x^*(t), u^*(t)) & & +L(x^*(t), u(t)). \end{array} \tag{32}$$

Based on the inequality of eq. (32), we have Theorem 4 and its proof shows the values of two optimal controls.

Theorem 4. *There exists two optimal controls $u_1^*(t)$ and $u_2^*(t)$ that maximize the objective function J over the region $\mathcal{U}$ is given by*

$$u_1^*(t) = \max_{[t_s,t_f]}\left\{\min\left\{-\frac{\tau p_B}{2A_2}, 1\right\}, 0\right\}$$
$$u_2^*(t) = \max_{[t_s,t_f]}\left\{\min\left\{\frac{\sigma p_B B(t)}{2A_3}, 1\right\}, 0\right\}$$

Proof. By optimality conditions, we have

$$\frac{\partial H}{\partial u_1(t)} = 0,$$
$$-2A_2 u_1 + \tau p_B = 0,$$
$$\therefore\ u_1(t) = \frac{\tau P_B}{2A_2},$$

and

$$\frac{\partial H}{\partial u_2(t)} = 0,$$
$$2A_3 u_2 = \sigma p_B B(t),$$
$$\therefore\ u_2(t) = \frac{\sigma p_B B(t)}{2A_3}.$$

According to the property of $\mathcal{U}$, the control $u_1^*(t)$ is bounded with upper bound 1 and lower bound 0. Therefore

$$u_1^*(t) = \begin{cases} 0 & ; \quad u_1 \leq 0 \\ \frac{\tau p_B}{2A_2} & ; \quad 0 < u_1 < 1 \\ 1 & ; \quad u_1 > 1 \end{cases}$$

This can be written in compact form as

$$u_1^*(t) = \max_{[t_s,t_f]}\left\{\min\left\{\frac{\tau p_B}{2A_2}, 1\right\}, 0\right\}$$

Similarly,

$$u_2^*(t) = \begin{cases} 0 & ; \quad u_1 \leq 0 \\ \frac{\sigma p_B B(t)}{2A_3} & ; \quad 0 < u_1 < 1 \\ 1 & ; \quad u_1 > 1 \end{cases}$$

leads to the compact form as

$$u_2^*(t) = \max_{[t_s,t_f]}\left\{\min\left\{\frac{\sigma p_B B(t)}{2A_3}, 1\right\}, 0\right\}$$

Thus, it completes the proof. □

5. Model Simulations and Discussion

The optimal solution of the controlled problem (eqs. (1) and (2)) has been formulated (see Section 4) and numerically computed using the forward-backward sweep method [32]. In a previous study related to this work [19], the first weight parameter in the objective function was set to $A_1 = 20$. Additionally, the weight parameters $A_2 = 220, A_3 = 300$ were chosen to reflect the cost per person for awareness campaigns and incentive programs, corresponding to 220 Taka and 300 Taka, respectively, in Bangladeshi currency. Therefore, the optimal numerical solution for the state and adjoint equations associated with the objective function has been obtained using MATLAB (R2021b). This calculation is based on the parameter values from Table 1, along with the corresponding weight parameters and initial conditions $N(0) = 126255.866$ (in thousands) and $B(0) = 7.493$ (per thousand) [19].

If the birth rate increases to $\tau = 0.0081$ and $\sigma = 0.0057$ due to incentives and awareness programs after 2023 keeping all other values the same as mentioned in Table 1 , the projected population will reach 1.06×10^5(in thousands), which is aligned with the predictions of The World Counts [33]. Now, we will explore different phenomena based on various cases of control strategies, analyzing their effects and implications.

Case-1 $\big(u_1(t) = 0.5$ and $u_2(t) = 0\big)$: Allocating 50% of Total Capacity to Awareness Programs Without Incentives

Figure 4 depicts a case where 50% of the total capacity is allocated to awareness programs, while no incentives are provided to increase the population growth rate. From Figures 4a and 4b,

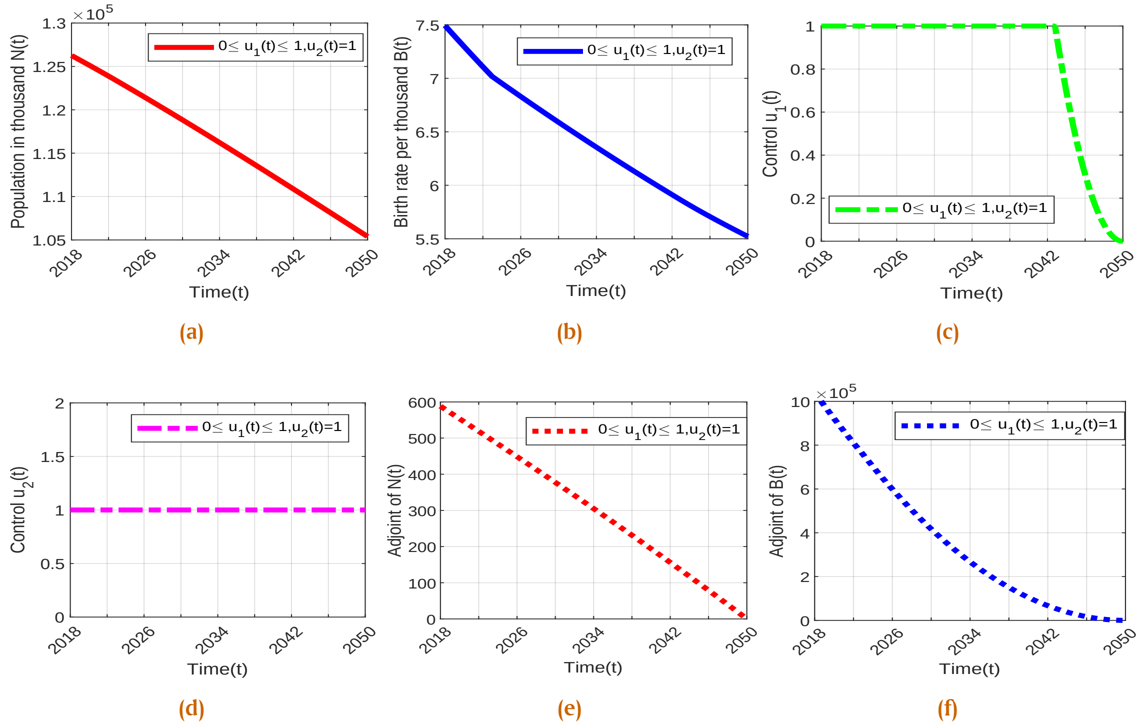

Figure 8. Impact of the optimal incentive strategy and full capacity utilization for awareness campaigns, as depicted in (c) and (d), on the simulated solution curves for population in Japan and birth rate in (a) and (b), respectively, with the corresponding adjoint profiles shown in (e) and (f). [Case-7]

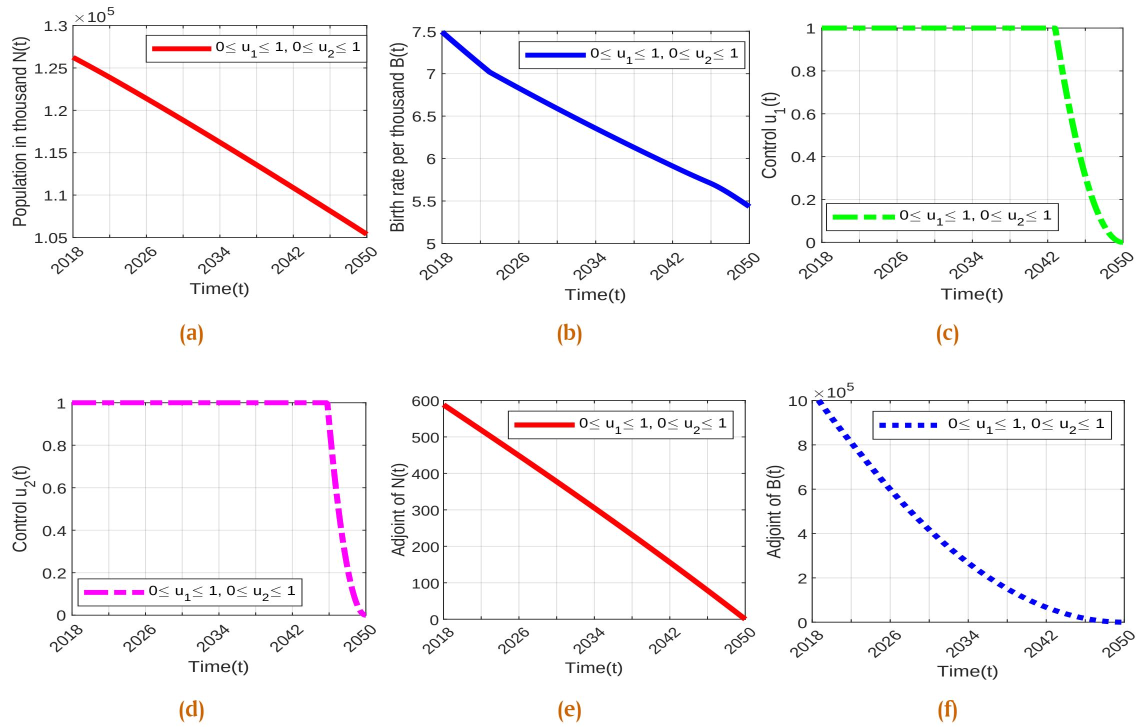

Figure 9. The implementation of an optimal strategy integrating awareness campaigns and incentives, as shown in (c) and (d), drives the simulated solution curves for population and birth rate in (a) and (b), while the corresponding adjoint profiles are depicted in (e) and (f). [Case-8]

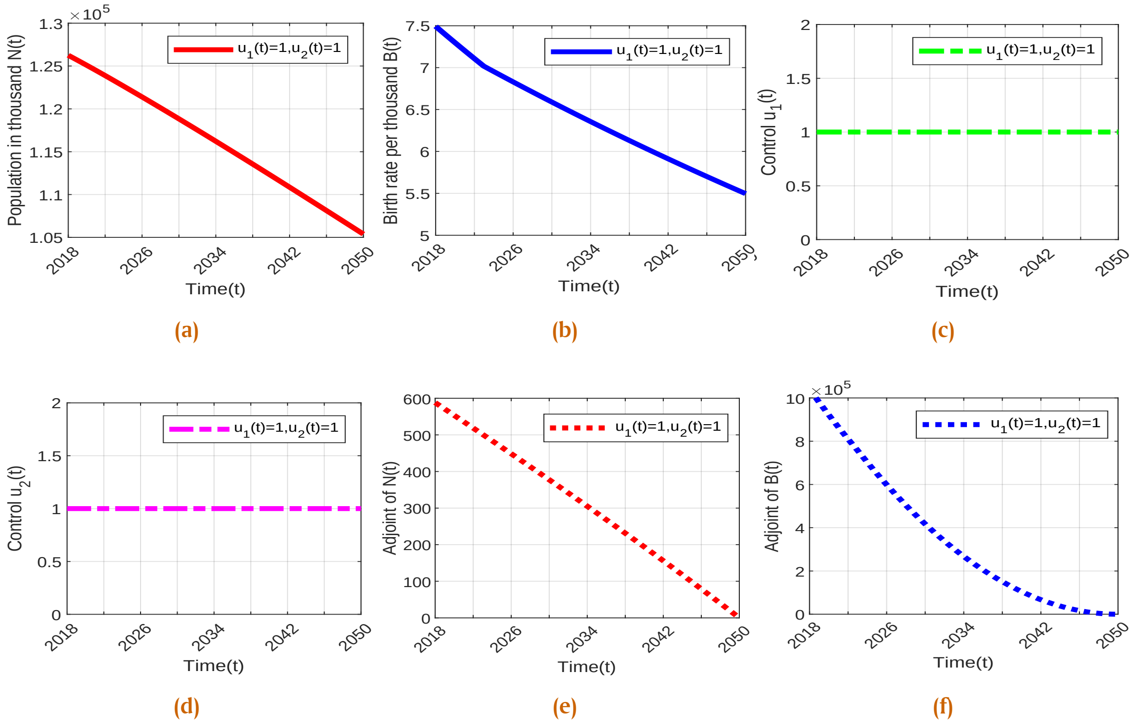

Figure 10. The full utilization of capacity for awareness campaigns and incentives, illustrated in (c) and (d), leads to the simulated solution curves for population and birth rate shown in (a) and (b), respectively, with the associated adjoint profiles displayed in (e) and (f). [Case-5]

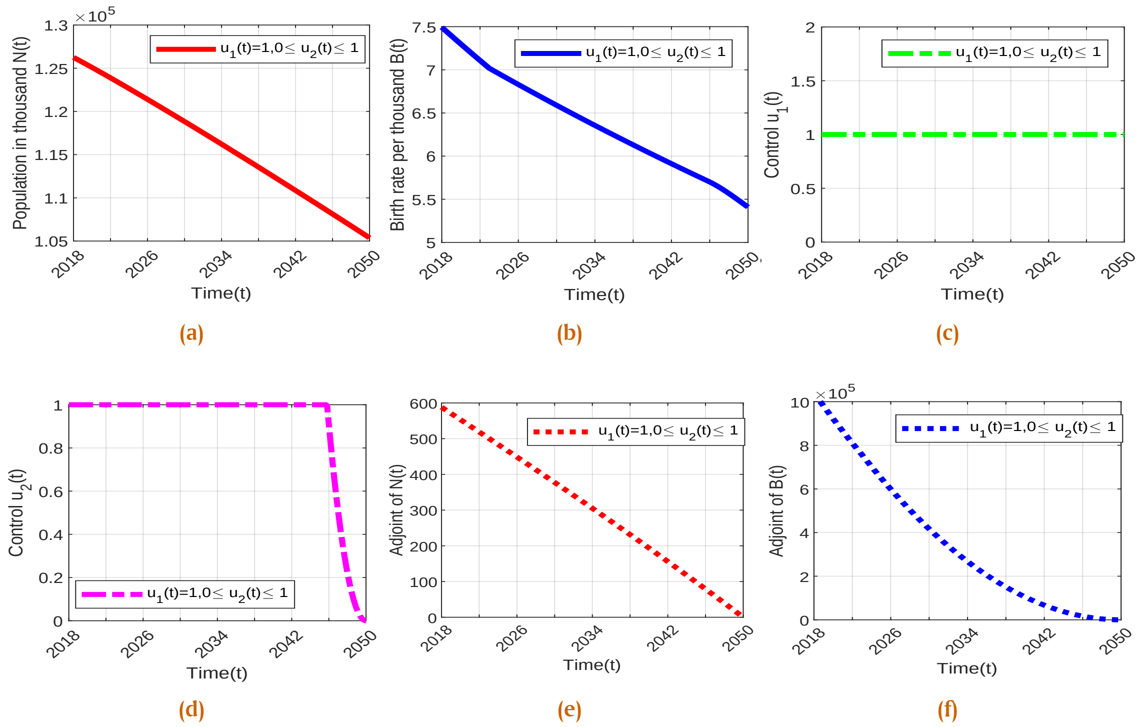

Figure 11. The complete utilization of capacity for awareness campaigns, combined with an optimal incentive strategy, as illustrated in (c) and (d), results in the simulated solution curves for population and birth rate presented in (a) and (b), respectively, with the corresponding adjoint profiles shown in (e) and (f). [Case-6]

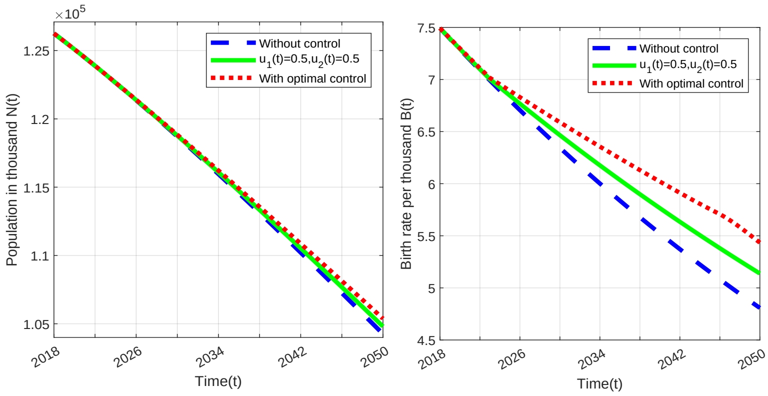

(a) (b)

Figure 12. Population in Japan as well as birth rate are increasing when both controls are optimal.

Table 2. Summary of Objective Functional

Case No	Status of Control	Value of Objective Functional	Population ($N(t)$)	Birth rate ($B(t)$)
1	$u_1(t) = 0.5; u_2(t) = 0$	7.4038×10^7	1.0414×10^5	4.7502
2	$u_1(t) = 0; u_2(t) = 0$	7.4065×10^7	1.0425×10^5	4.8073
3	$u_1(t) = 0.5; u_2(t) = 0.5$	7.4176×10^7	1.0480×10^5	5.1378
4	$u_1(t) = 0; u_2(t) = 0.5$	7.4203×10^7	1.0492×10^5	5.2077
5	$u_1(t) = 1; u_2(t) = 1$	7.4282×10^7	1.0538×10^5	5.4961
6	$u_1(t) = 1; 0 \leq u_2(t) \leq 1$	7.4283×10^7	1.0537×10^5	5.4086
7	$0 \leq u_1(t) \leq 1; u_2(t) = 1$	7.4284×10^7	1.0539×10^5	5.5215
8	$0 \leq u_1(t) \leq 1; 0 \leq u_2(t) \leq 1$	$\mathbf{7.4285 \times 10^7}$	1.0538×10^5	5.4338

Table 3. Control strategies in ascending order of net gain in population

(A1)	(A2)	(A3)	(A4)	A(5)
Strategy	Total Cost for Policy (TC)	Population with control	Population without control	Net Gain (TA) (A3-A4)
C_{Aw}	5.7598×10^3	7.4014×10^7	7.4065×10^7	-0.0051×10^7
C_{In}	8.6021×10^3	7.4352×10^7	7.4065×10^7	0.0287×10^7
C_{AwIn}	1.4365×10^4	7.4299×10^7	7.4065×10^7	0.0234×10^7

it is observed that the population gradually declines, reaching less than 1.05×10^5 by 2025, with the birth rate decreasing from 7.493 to 4.746. Additionally, the adjoint states reach zero at the final time, confirming that the transversality condition (28) of the maximum principle is satisfied for the optimally controlled problem.

Case-2$(u_1(t) = 0$ and $u_2(t) = 0)$: No Focus on Awareness Programs or Incentives

In the scenario depicted in Figure 4, neither awareness programs nor incentives are implemented, leading to a significant effect on the state variables. The decline in both birth rate and overall population is significantly steeper compared to the previous case, highlighting the crucial role of strategic interventions. Notably, at the final time, the adjoint states reach zero, indicating that the transversality condition of the maximum principle is satisfied for the optimally controlled problem (see eq. (28)).

Case-3 $(u_1(t) = 0.5$ and $u_2(t) = 0.5)$: Allocating 50% of Total Capacity to Awareness Programs as well as Incentives Providing Strategy

In the case illustrated in Figure 6, half of the total capacity is dedicated to organizing awareness programs and providing incentives to support population growth. The simulation results, illustrated in Figures 6a and 6b, demonstrate the effects of this intervention on population and birth rate trends. Although this partial allocation helps mitigate the decline, the reduction in both population and birth rate remains significant higher compared to previously described cases. The control strategies are depicted in Figures 6c and 6d, while the corresponding adjoint profiles in Figures 6e and 6f confirm that the adjoint states reach zero at the final time, ensuring compliance with the transversality condition of the maximum principle (as mentioned in eq. (28)).

Case-4 $(u_1(t) = 0.5$ and $u_2(t) = 0.5)$: Allocating 50% of Total Capacity to Incentives without Arranging Awareness Programs

Figure 7 illustrates a scenario where 50% of the total capacity is allocated exclusively to providing incentives, with no awareness programs in place. As shown in Figures 7a and 7b, it is observe that while incentives alone have some effect on mitigating the decline, their impact is less substantial compared to more holistic strategies, though this time the population was higher that last three cases. Over a span of 32 years, the birth rate decreases from 7.4 to 5.2, corresponding to a reduction of approximately 29.73%. This significant decline emphasizes the limitations of relying solely on incentives, highlighting the need for

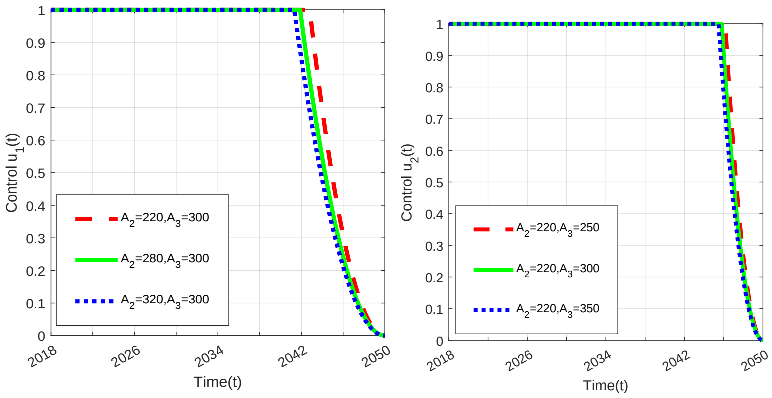

(a) (b)

Figure 13. Control dynamics of (a) $u_1(t)$ and (b) $u_2(t)$ under different weight parameter values.

Table 4. ICER values of Control strategies C_{In} and C_{Aw}

Strategy	Total Cost for Policy (TC)	Net Gain Population (TA)	ICER
C_{In}	8.6021×10^3	0.0287×10^7	0.0299725
C_{Aw}	5.7598×10^3	-0.0051×10^7	0.0084091

Table 5. ICER values of Control strategies C_{Aw} and C_{AwIn}

Strategy	Total Cost for Policy (TC)	Net income (TA)	ICER
C_{Aw}	5.7589×10^3	-0.0051×10^7	-0.11294
C_{AwIn}	1.4365×10^4	0.0234×10^7	0.03019

a more integrated approach that combines both incentives and awareness programs. At the same time, the control strategies in Figures 7c and 7d, along with the adjoint profiles in Figures 7e and 7f, confirm that the adjoint states reach zero at the final time, satisfying the transversality condition of the maximum principle for this optimal control problem.

Case-5$\big(u_1(t) = 0$ and $u_2(t) = 0\big)$: Full Deployment of Capacity for Awareness Campaign and Incentives

In the scenario of full deployment of capacity for awareness campaigns and incentives (from Figure 10), the birth rate decreases from 7.4 to 5.5 over the 32-year period. The control strategies along with the adjoint profiles show that the adjoint states reach zero at the final time, fulfilling the transversality condition (see eq. (28)). Thus, the adherence of the adjoint states to the transversality condition confirms the optimality of the applied strategies in achieving the desired demographic outcome.

Case-6$\big(u_1(t) = 1$ and $0 \leq u_2(t) \leq 1\big)$: Full Capacity Allocation for Arranging Awareness Programs with an Optimal Control Strategy for Incentives

Figure 11 explores a scenario where incentives are provided at their optimal level while the full capacity is allocated to awareness campaigns, maintaining a strategy similar to the previous case. The results indicate a continuous decline in both population and birth rate from 2023 to 2047, with a slightly sharper reduction observed after this period (2047) compared to earlier cases (see Figures 11a and 11b). A closer examination of the control profile for u_2 reveals that incentives should be maintained at near-full capacity until 2046, after which a gradual reduction is necessary (Figure 11d). Meanwhile, $u_1(t)$ remains at 1 throughout, as depicted in Figure 11c, signifying the continuous full deployment of awareness programs. Furthermore, the adjoint profiles in Figures 11e and 11f confirm that the transversality condition of the maximum principle is met, validating the effectiveness of the applied control strategy in managing demographic trends.

Case-7$\big(0 \leq u_1(t) \leq 1$ and $u_2(t) = 1\big)$:Optimal Strategy for Awareness Programs with Full Ability of Offerering Incentives

Figure 8 presents an just opposite strategy to the previous scenario, where awareness campaigns are maintained at their optimal level while the entire capacity is allocated to providing incentives. This approach examines the impact of prioritizing financial support over informational outreach, offering insights into the effectiveness of different resource allocation strategies in influencing population and birth rate trends.

Case-8$\big(0 \leq u_1(t) \leq 1$ and $0 \leq u_2(t) \leq 1\big)$: Optimal Strategy for Awareness Programs and Incentive Offerings

A strategic approach to increasing population growth can be most effective if the expenditures on awareness programs and incentive offerings are optimized. Figure 9 illustrates the scenario where control profiles, u_1 and u_2, are optimally implemented. Figures 9a and 9b depict the population and birth rate dynamics under optimal cost control and resource allocation, ensuring maximum profitability. Furthermore, as observed in Figures 9c and 9d, achieving maximum profitability requires the full utilization of available capacity for awareness programs and incentives until 2042 and 2046, respectively. Beyond this period, a gradual reduction in expenditures is necessary for sustaining long-term benefits and maintaining an optimal population level.

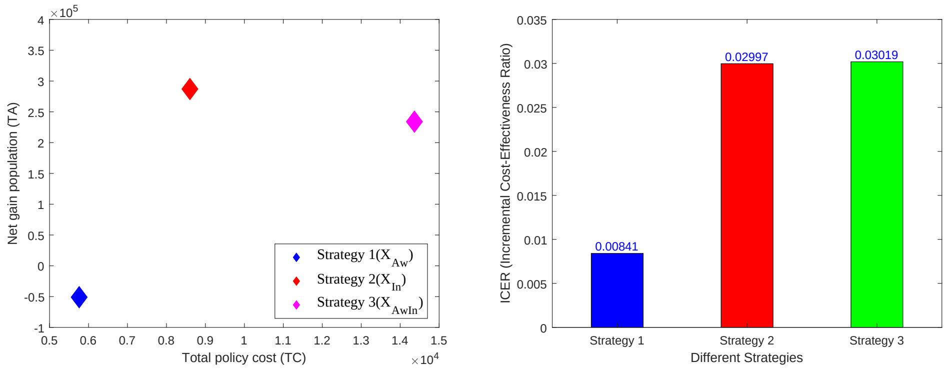

(a) (b)

Figure 14. Comparison of policy impact and cost-effectiveness for different strategies: (a) total policy cost vs. net population gain and (b) ICER values for three strategies.

Finally, Figures 9e and 9f present the adjoint profiles, confirming that the transversality condition of the maximum principle (eq. (28)) is satisfied, as the adjoint states reach zero at the final time.

However, Figure 12 illustrates that the population and birth rate in Japan reach their highest levels at the final time when both control variables, $u_1(t)$ and $u_2(t)$, are applied optimally. This indicates that optimal utilizing awareness programs and incentives leads to the most favorable demographic outcomes. In contrast, when both controls are set to a constant value of $u_1(t) = u_2(t) = 0.5$, the population and birth rate remain at intermediate levels, suggesting that partial implementation of these strategies results in a moderate impact on demographic trends.

In a nutshell, Table 2 describes a comparative analysis of different control strategies in optimizing population growth and birth rate in Japan. It evaluates various cases based on the values of the control variables $u_1(t)$ (awareness programs) and $u_2(t)$ (incentives), along with their impact on the objective functional, population, and birth rate. From this table, it is seen that in Case 1, where $u_1(t) = 0.5$ and $u_2(t) = 0$, the population is 1.0141×10^5 with the lowest birth rate (4.7502) and an objective value of 7.4038×10^7. In Case 2, with awareness at zero and incentives fully applied ($u_1(t) = 0, u_2(t) = 1$), the birth rate increases to 4.8703, and the population grows to 1.0425×10^5, leading to a slightly improved objective value of 7.4065×10^7. Case 3, where awareness remains absent while incentives are reduced to 50% ($u_1(t) = 0, u_2(t) = 0.5$), results in a population of 1.0480×10^5 and a birth rate of 5.1378, increasing the objective value to 7.4176×10^7. When awareness is applied at 50% and incentives are at full capacity always ($u_1(t) = 0.5, u_2(t) = 1$, Case 4), the birth rate slightly decreases to 5.2077, while the population remains nearly the same at 1.0492×10^5, yielding an objective value of 7.4203×10^7. Case 5, where awareness is fully implemented and incentives are absent ($u_1(t) = 1, u_2(t) = 0$), leads to a significant population increase (1.0538×10^5) with a birth rate of 5.4961, reaching an objective value of 7.4282×10^7. When awareness is absent and incentives are at full capacity ($u_1(t) = 0, u_2(t) = 1$, Case 6), the population reaches 1.0537×10^5 with the birth rate (5.4086), slightly decreasing the objective value to 7.4283×10^7. Case 7 introduces partial control variations ($0 \leq u_1(t) \leq 1, u_2(t) = 1$), resulting in the highest birth rate of 5.5215 and maintaining a high population level but the objective functional value is not the highest among all. Finally, Case 8, where both controls vary optimally within their full range ($0 \leq u_1(t) \leq 1, 0 \leq u_2(t) \leq 1$), achieves the highest objective functional value (7.4285×10^7), confirming that adaptive control strategies lead to the best outcomes.

The impact of rising control costs on the variation in control profiles is depicted in Figure 13. The observed trend indicates that as the expenditure on awareness programs and incentive schemes increases, the full capacity of the application decreases, emphasizing the importance of strategic resource allocation for optimal implementation

6. Cost-effectiveness Analysis

Selecting the most cost-effective optimal control strategy from various single and combined techniques is crucial for maximizing Japan's population. Cost-effectiveness analysis helps quantify the economic benefits of each strategy by comparing their costs and outcomes. This study provides a detailed evaluation using the Incremental Cost-Effectiveness Ratio (ICER) to assess the efficiency of different approaches [30, 34–37], which assesses the variances between the policy costs and outcomes (maximum possible population of Japan) of two competing strategies for intervention.

Let, three strategies C_{Aw} (Strategy 1), C_{In} (Strategy 2) and C_{AwIn} (Strategy 3) represent the control strategies for organizing awareness campaigns, offering incentives to married couples, and a combination of these two strategies, respectively. The ICER is defined as the quotient of the difference in costs in strategies i and j, by the difference in net income in strategies i and $j (i, j \in \{1, 2, 3\})$.

In general formula: Given two competing strategies X_1 and X_2, where strategy X_2 has higher effectiveness than strategy X_1 $\Big(TA(X_2) > TA(X_1)\Big)$, the ICER values are calculated as follows:

$$ICER(X_1) = \frac{TC(X_1)}{TA(X_1)}$$

Table 6. Comparison of related studies and the present work, highlighting its novelty

Study	Methodology	Region	Focus Area	Novelty
Oizumi et al. [17]	Multi-regional Leslie matrix model with sensitivity analysis	Japan, focusing on urban and non-urban prefectures	Domestic factors driving population decline (fertility, migration, regional traits)	New method connecting reproductive value and stable age distribution to matrix entries, with genealogical interpretation
Oliver [18]	Econometric analysis of demographic composition and immigration trends from 1975–2019	Japan	Relationship between aging population structure and increase in immigration rates	Identifies specific age group dynamics (60–64, 65+) influencing immigration patterns in Japan through long-term data analysis
Inoue and Inoue [20]	Quantitative analysis using SAPP for Japan data, non-hierarchical cluster analysis, and stage-based demographic modeling	Japan, focusing on small-area populations and aging trends	Future aging processes, demographic transition stages, and regional aging patterns	First nationwide study using small-area projections to model aging stages, with generalizable findings for other developed countries post-demographic transition
Kundu and Mallick [19]	Dynamical System using ODE and Runge Kutta 4th order simulation method	Japan	Impact of declining birth rates on social structure, economy, and family planning	Newly proposed dynamic model taking birth rate as a variable, linking demographic decline to economic and social awareness as well as incentive needs
Present Study	Optimal control model analyzed using Pontryagin's Maximum Principle with cost-effectiveness evaluation	Japan, focusing on national demographic trends	Strategies for boosting birth rate through awareness programs and incentives while minimizing costs	Finding optimal control strategy of awareness programs and incentives for maximizing population considering optimum cost, cost-effectiveness analysis is evaluated to raise Japan's fertility trend

$$ICER(X_2) = \frac{TC(X_2) - TC(X_1)}{TA(X_2) - TA(X_1)}$$

where the total policy costs (TC) and the net population of Japan (TA) are defined, during a given period for strategies X_i for $i = 1, 2, 3$ by:

$$TC(X_i) = \int_{t_s}^{t_f} \Big[A_2 u_1^2(t) + A_3 u_2^2(t)\Big] dt$$
$$TA(X_i) = \int_{t_s}^{t_f} \Big[\Big(A_1 N^*(t)\Big) - \Big(A_1 N(t)\Big)\Big] dt$$

where $\big(A_1 N^*(t)\big)$ indicates the optimal solution associated with the optimal control, u_1^*, u_2^*. where solution without the corresponding control strategy is denoted by $\big(A_1 N(t)\big)$. Based on the numerical simulation results, we listed our control strategies in Table 3 according to their ability to rise the population of Japan.

Based on the data shown in Table 3, it can be concluded that the combined strategy C_{AwIn} shows higher total costs for policy and net gain population with control compared to the individual strategies C_{Aw} and C_{In}. However, the net population gain without control remains the same for all strategies. Simultaneously, this table also demonstrates that the net gain for strategy C_{In} is greater than that of strategies C_{Aw} and C_{AwIn}.

Now, we compute and compare the strategy C_{In} with the strategy C_{Aw} as shown in Table 4. The ICER of C_{In} and C_{Aw} are calculated as follows:

$$ICER(C_{In}) = \frac{TC(C_{In})}{TA(C_{In})} = 0.0299725$$
$$ICER(C_{Aw}) = \frac{TC(C_{Aw}) - T(C_{In})}{TA(C_{Aw}) - TA(C_{In})} = 0.0084091$$

Comparing strategies C_{In} and C_{Aw} we see that $ICER(C_{Aw}) < ICER(C_{In})$. This highlights that strategy C_{In} is more expensive and less effective than strategy C_{Aw}. Next, the strategy C_{Aw} is compared to the strategy C_{AwIn} mentioned in Table 5. The ICER values for these strategies are calculated below:

$$ICER(C_{Aw}) = \frac{TC(C_{Aw})}{TA(C_{In})} = -0.11294$$
$$ICER(C_{AwIn}) = \frac{TC(C_{AwIn}) - TC(C_{Aw})}{TA(C_{AwIn}) - TA(C_{Aw})} = 0.03019$$

Based on the comparison of the ICER values of C_{Aw} and C_{AwIn}, it can be said that strategy C_{Aw} is both less expensive and more efficient than strategy C_{AwIn}. In short, Figure 14a showcases the trade-off between total policy cost (TC) and net population gain (N), revealing that strategies with higher investments yield greater benefits. But, at the same time, Figure 14b compares the incremental cost-effectiveness ratio (ICER) of three strategies, showing that Strategy 1 is the most cost-effective, whereas Strategies 2 and 3 incur higher costs for similar effectiveness.

Thus, it can be concluded that the strategy C_{Aw} has the potential to exhibit greater effectiveness and cost efficiency than other approaches in increasing Japan's population. In short, Strategy 1 (organizing awareness campaigns C_{Aw}) is the most cost-effective because it mainly relies on communication tools like media, workshops, and community outreach, which can reach a large audience at a relatively low cost. On the other hand, Strategy 2 (offering incentives C_{In}) and Strategy 3 (combining awareness with incentives C_{AwIn}) require significant financial investment for the incentives themselves, making them more expensive to implement and maintain. However, Table 6 provides a comparison of related studies and the present work, emphasizing the novel aspects and first-time contributions of this study.

7. Conclusions

This study examined the impact of awareness programs and financial incentives on population growth dynamics in Japan over a specified time period. To achieve this, a newly formulated optimal control problem was formulated using a system of nonlinear differential equations including two control variables. Following the qualitative analysis, the optimal control strategies were characterized through Pontryagin's maximum principle, ensuring the identification of adjoint variables and the existence of optimal controls. The numerical simulations explored eight distinct cases, revealing different outcomes, each illustrating the varying effects of policy interventions.

The findings indicate that implementing both control strategies optimally can significantly enhance Japan's birth rate. Notably, the control profile adapts dynamically to changes in cost, suggesting that increased investment in these interventions becomes more likely as their costs rise. Moreover, the cost-effectiveness analysis highlights that an optimally managed awareness program policy outperforms both individual and combined strategies in maximizing long-term benefits.

Overall, this study underscores the importance of proactive policy interventions, demonstrating how a strategic balance between incentives and awareness programs can effectively influence demographic trends. Real-world implementations of these strategies could provide deeper insights into their long-term efficacy in addressing Japan's declining birth rate. Future research can extend this study by incorporating fractional-order derivatives in the model to better capture memory effects and hereditary properties in birth rate dynamics.

Author Contributions. **Kundu, P.**: Conceptualization, investigation, formal analysis, methodology, data collection, software, visualization, Writing –original draft preparation, writing –review and editing. **Mallick, U. K.**: Conceptualization, formal analysis, methodology, data curation, software, visualization, writing –review and editing, supervision, Validation.

Acknowledgement. The authors sincerely thank the editors and reviewers for their constructive feedback and valuable guidance in enhancing the quality of this manuscript.

Funding. This research received no external funding.

Conflict of interest. The authors declare that they have no known competing financial interests or personal relationships that could have appeared to influence the work reported in this study.

Data availability. The data used to support the findings of this study are included in the manuscript.

References

[1] IFO and Sakura Institute of Research, *"A Comparative Analysis of Japanese and German Economic Success"*, 1st ed., ser. Springer Book Archive. Springer Tokyo, 1997, ISBN 978-4-431-65867-2. DOI:10.1007/978-4-431-65865-8

[2] K. Ohno, *The History of Japanese Economic Development: Origins of Private Dynamism and Policy Competence*, 1st ed. London: Routledge, 2017. DOI:10.4324/9781315444048

[3] G. Nargund, "Declining birth rate in developed countries: A radical policy re-think is required," *Facts, Views & Vision in ObGyn*, vol. 1, no. 3, pp. 191–193, 2009.

[4] nippon.com., "Japan's fertility rate drops to new record low," https://www.nippon.com/en/japan-data/h02015/, Accessed on March 14 2025.

[5] E. Yokoyama, "Japan records fewest births on record, deepening demographic crisis," 2025, https://www.japantimes.co.jp/news/2025/02/27/japan/fewest-births-new-record/, Accessed on March 14 2025.

[6] ALJazeera, "Japan's elderly population rises to record 36.25 million," 2024, https://www.aljazeera.com/economy/2024/9/16/japans-elderly-population-rises-to-record-36-25-million, Accessed on March 14 2025.

[7] M. Yamaguchi. "Japan's birth rate fell for a ninth consecutive year in 2024 to hit a record low," 2025, https://apnews.com/article/japan-births-children-population-decline-marriage-37c1a83afb9f90c6ce6affd527829826, Accessed on March 14 2025.

[8] K. Alexander, "The demographic deficit: National security challenges for japan and south korea," 2024, https://www.isdp.eu/the-demographic-deficit-national-security-challenges-for-japan-and-south-korea/, Accessed on March 14 2025.

[9] S. I. Fukuda and K. Okumura, "The aging society, savings rates, and regional flow of funds in japan," *Journal of the Japanese and International Economies*, vol. 62, p. 101165, 2021. DOI:10.1016/j.jjie.2021.101165

[10] H. Faruqee and M. Mühleisen , "Population aging in japan: Demographic shock and fiscal sustainability," *Japan and the World Economy*, vol. 15, no. 2, pp. 185–210, 2003. DOI:10.1016/S0922-1425(02)00017-8

[11] H. Arai *et al.*, "Japan as the front-runner of super-aged societies: Perspectives from medicine and medical care in japan," *Geriatrics & Gerontology International*, vol. 15, no. 6, pp. 673–687, 2015. DOI:10.1111/ggi.12450

[12] M. Rahman, "All initiatives of the japanese government to increase the population," 2023, https://bangla.thedailystar.net/abroad/news-440531, Accessed on March 10 2025.

[13] A. Mahdy, N. Sweilam, and M. Khader, "Numerical simulation for the fractional sirc model and influenza a," *Applied Mathematics & Information Sciences An International Journal*, vol. 8, no. 3, pp. 1–8, 2014. DOI:10.12785/amis/080311

[14] F. Akbar and Mardlijah, "Optimizing algal bloom through bioenzyme and harvesting control for bioenergy purposes in eutrophic water bodies," *Jambura Journal of Biomathematics*, vol. 5, no. 2, pp. 109–115, 2024. DOI:10.37905/jjbm.v5i2.26938

[15] P. Luis *et al.*, "Implementation of non-standard finite difference on a predator-prey model considering cannibalism on predator and harvesting on prey," *Jambura Journal of Biomathematics*, vol. 6, no. 1, pp. 35–43, 2025. DOI:10.37905/jjbm.v6i1.30550

[16] T. P. Blante, Jaharuddin, and E. H. Nugrahani, "Sensitivity analysis of si1i2rs model for dengue fever transmission," *Jambura Journal of Biomathematics*, vol. 5, no. 1, pp. 19–26, 2024. DOI:10.37905/jjbm.v5i1.23132

[17] R. Oizumi *et al.*, "Sensitivity analysis on the declining population in japan: Effects of prefecture-specific fertility and interregional migration," *PloS One*, vol. 17, no. 9, p. e0273817, 2022. DOI:10.1371/journal.pone.0273817

[18] M. Oliver, "Population aging and immigration: Evidence from japan," *International Journal of Population Studies*, vol. 9, no. 1, pp. 18–29, 2023.

DOI:10.36922/ijps.407

[19] P. Kundu and U. K. Mallick, "Mathematical modeling and analysis on the population birth rate trends in japan," *Journal of Mathematics*, vol. 2024, no. 1, p. 2246763, 2024. DOI:10.1155/jom/2246763

[20] T. Inoue and N. Inoue, "The future process of japan's population aging: A cluster analysis using small area population projection data," *Population Research and Policy Review*, vol. 43, p. 58, 2024. DOI:10.1007/s11113-024-09903-5

[21] F. Respatiadi, M. Jalaluddin, and A. Munandar, "Strategy for overcoming population growth problems in japan," *Al Qalam: Jurnal Ilmiah Keagamaan dan Kemasyarakatan*, vol. 18, no. 03, pp. 1978–1996, 2024. DOI:10.35931/aq.v18i3.3498

[22] S. Kim, Y. Lee, and H. Oh, "Estimation of gridded population with spatial downscaling in south korea," *Sustainability*, vol. 17, no. 4, p. 1511, 2025. DOI:10.3390/su17041511

[23] P. Samui *et al.*, "Impact of awareness in self–monitoring of covid-19: An optimal control approach," *Results in Control and Optimization*, vol. 18, p. 100513, 2025. DOI:10.1016/j.rico.2024.100513

[24] F. I. Igbo, K. Gossett, and D. Nattress, "Strategies for cost-effectiveness in sustainable quality healthcare delivery in emerging economies: The case of healthcare professionals development in south africa," *Healthcare*, vol. 13, no. 1, p. 36, 2025. DOI:10.3390/healthcare13010036

[25] W. Fleming and R. Rishel, *Deterministic and Stochastic Optimal Control*, 1st ed. Berlin: Springer-Verlag, 1975, ISBN 0387901558. DOI:10.1007/978-1-4612-6380-7

[26] L. S. Pontryagin *et al.*, *Mathematical Theory of Optimal Processes*, 4th ed. New York: Wiley-Interscience, 1962.

[27] R. Vinter, *Deterministic and Stochastic Optimal Control*. Boston: Birkhauser, 2010, vol. 2, no. 1, ISBN 0387901558. DOI:10.1007/978-1-4612-6380-7

[28] H. Anton, I. Bivens, and S. Davis, *Calculus*, 10th ed. United States of America: Wiley, 2012, chapter 13: Partial Derivatives.

[29] S. Sowole *et al.*, "On the existence, uniqueness, stability of solution and numerical simulations of a mathematical model for measles disease," vol. 2019, pp. 84–111, 2019.

[30] P. Kundu and U. K. Mallick, "Optimal control analysis of a mathematical model for guava nutrients in an integrated farming with cost-effectiveness," *Results in Control and Optimization*, vol. 17, p. 100490, 2024. DOI:10.1016/j.rico.2024.100490

[31] M. A. Omoloye and S. O. Adewale, "Mathematical analysis of sensitive parameters on the dynamical transmission of ebola-malaria coinfections," *International Journal of Computer Science and Information Security (IJCSIS)*, vol. 19, no. 7, pp. 21–45, 2021.

[32] S. Lenhart and J. T. Workman, *Optimal Control Applied to Biological Models*, 1st ed. New York: Taylor and Francies Group, 2007. ISBN 9780429138058

[33] The World Counts, "Population of japan," https://www.theworldcounts.com/populations/countries/japan, Accessed on March 14 2025

[34] A. Kouidere, O. Balatif, and M. Rachik, "Cost-effectiveness of a mathematical modeling with optimal control approach of spread of covid-19 pandemic: A case study in peru," *Chaos, Solitons & Fractals: X*, vol. 10, p. 100090, 2023. DOI:10.1016/j.csfx.2022.100090

[35] A. Venkatesh and M. A. Rao, "Mathematical model for covid-19 pandemic with implementation of intervention strategies and cost-effectiveness analysis," *Results in Control and Optimization*, vol. 14, p. 100345, 2024. DOI:10.1016/j.rico.2023.100345

[36] Z. Chazuka, C. E. Madubueze, and D. Mathebula, "Modelling and analysis of an hiv model with control strategies and cost-effectiveness," *Results in Control and Optimization*, vol. 14, p. 100355, 2024. DOI:10.1016/j.rico.2023.100355

[37] S. Al-Shanfari *et al.*, "Mathematical analysis and optimal control of cholera–malaria co-infection model," *Results in Control and Optimization*, vol. 14, p. 100393, 2024. DOI:10.1016/j.rico.2024.100393